Calculation of RMS Values for Variable Frequency Sinusoidal Signals, Using Phasors and Digital SAL and CAL Filters

Yonatan AGUIRRE[a], Flabio GUTIERREZ[b,1], Richard ABRAMONTE[b], Nilthon ARCE[c] and Antenor ALIAGA[a]

[a]*Department of Electronics, Universidad Nacional de Piura, Piura, Peru*
[b]*Department of Mathematics, Universidad Nacional de Piura, Piura, Peru*
[c]*Department of Civil Engineering, Universidad Nacional de Jaen, Cajamarca, Peru*

Abstract. The accurate measurement of RMS values of voltage and current is crucial for the monitoring and protection of power systems and in general for electrical power distribution systems. The authors in this paper have developed an algorithm to calculate the RMS value of sinusoidal signals of varying frequency, by applying phasors obtained from digital filters SAL and CAL. In conditions in which the frequency of the grid varies, a phase shift is presented in the phasor of the grid voltage which is used for the design of a regulator that allows to obtain accurate RMS voltage values. The choice of the SAL and CAL digital filters is due to their low computational requirement, so they can be implemented in general-purpose microcontrollers.

Keywords. RMS, phasors, digital filters, regulators

1. Introduction

The accurate measurement of RMS voltage and current values is crucial for the monitoring and protection of power systems and power distribution systems in general. One of the applications in which it is necessary to measure RMS voltage (V_{RMS}) in a simple and accurate way is smart grids, which are a reliable supply of energy [1]. The applications include, in addition to transmission lines, the load monitoring in smart homes and industries ([2], [3]) and power quality estimation [4].

Among the alternating current (AC) measurement techniques, the digital sampling technique is the most widely used. The input signal is digitized using an analog-to-digital converter (ADC) and the RMS value of the signal is calculated using a digital signal processor (DSP). The achievable accuracy for any given bandwidth varies with the accuracy of the ADC and the sampling rate [5].

The implementation of the algorithm based on the mathematical definition of RMS in general-purpose microcontrollers requires of complex operations that imply a high

---

1 Corresponding Author: Flabio Gutierrez, Department of Mathematics, Universidad Nacional de Piura, Campus Universitario, Urb. Miraflores s/n, Castilla, Piura, Perú; E-mail: flabio@unp.edu.pe.

computational cost. Although some microcontrollers already integrate hardware to perform floating-point multiplication and division operations, in many cases other platforms are selected to implement mathematical tools to improve the performance of these operations ([6], [7]).

In real-time systems that require measuring RMS values as in ([8] - [10]), it is necessary to explore other algorithms that allow accurate measurements and have: low complexity, low computational cost and do not require specialized hardware; one of them is described in [11], which presents an algorithm to accurately obtain the V_{RMS} of the electrical grid, using phasors obtained by applying the digital signals processing techniques, specifically, using digital filters SAL and CAL.

The accuracy of the V_{RMS} values obtained by applying these filters requires that the selected sampling frequency is four times the frequency of the power grid. In this context, in environments where the frequency of the network presents variations and maintaining a constant sampling frequency, the above-mentioned requirement is not fulfilled, therefore, the V_{RMS} values obtained are not accurate.

This paper presents a new algorithm that uses the voltage phasor phase shift; because of the variations of the grid frequency, and a regulator to adjust the sampling frequency to four times the grid frequency, to fulfill the condition mentioned in the previous paragraph and to get accurate V_{RMS} values. Once the sampling time is adjusted, the actual grid frequency can be estimated.

Section two defines the SAL and CAL filters and the calculation of the V_{RMS} value. Section three covers the analysis of the accuracy of V_{RMS} values due to mains frequency variation and the relationship between phasor phase variation and line frequency variation. Section four describes the design of the regulator for the sampling frequency adjustment and finally in section five we show the results of the obtained V_{RMS} values as well as the estimated network frequency.

2. Preliminaries

2.1. Definition of RMS value

The mathematical definition of RMS of a signal x(t) is given by equation (1)

$$X_{RMS} = \sqrt{\frac{1}{T}\int_0^T x^2(t)dt} \tag{1}$$

Where T is the period of the signal.

2.2. Phasor of a sinusoidal signal

Given a sinusoidal signal represented by equation (2)

$$v(t) = V_m sin(w * t + \varphi) \tag{2}$$

Their phasor expressed in Cartesian form is given by the equation (3)

$$\boldsymbol{V} = V_m cos(\varphi) + jV_m \sin(\varphi) \tag{3}$$

And its representation in polar form is given by equation (4)

$$V = V_m \angle \varphi \tag{4}$$

Where:
V_m: maximum value of the sinusoidal signal.
φ: phase of the phasor for $t = 0$

2.3. Calculation of the phasor of v(t) using SAL and CAL filters

Given a sinusoidal signal of amplitude V_m, with line frequency F_L and phase φ, defined by equation (5)

$$v(t) = V_m sin(2 * \pi * F_L * t + \varphi) \tag{5}$$

Discretizing (5) by $t = k * T_s$, $\forall k \in \mathbb{Z}$, where $T_s = 1/F_s$ is the sampling time. For a sampling frequency F_s defined by equation (6), we obtain equation (7)

$$F_s = 4 * F_L \tag{6}$$

$$v(k) = V_m sin(\tfrac{\pi}{2} * k + \varphi) \tag{7}$$

Using the finite impulse response filters (FIR), whose coefficients are defined by the second and third one-dimensional Walsh functions [12], designed SAL and CAL by Harmuth (1969) and used in [11], we have:

$$SAL = v(k) + v(k-1) - v(k-2) - v(k-3) \tag{8}$$

$$CAL = v(k) - v(k-1) - v(k-2) + v(k-3) \tag{9}$$

by replacing (7) in (8) and (9) we get

$$SAL = -2\sqrt{2}\, V_m\, cos(\tfrac{\pi}{2} * k + \varphi + \tfrac{\pi}{4}) \tag{10}$$

$$CAL = 2\sqrt{2}\, V_m\, sin(\tfrac{\pi}{2} * k + \varphi + \tfrac{\pi}{4}) \tag{11}$$

Making

$$\phi = \tfrac{\pi}{2} * k + \varphi + \tfrac{\pi}{4} \tag{12}$$

And knowing that $V_m = V_{RMS}\sqrt{2}$ and (12), (10) and (11) can be written as:

$$SAL = -4V_{RMS}\, cos\, \phi \tag{13}$$

$$CAL = 4V_{RMS}\, sin\, \phi \tag{14}$$

Using (13) and (14) we can express the phasor X by the following equation

$$X = -SAL + j(CAL) \tag{15}$$

and its representation in polar form is given by the equation (16)

$$X = 4V_{RMS}\angle\phi \tag{16}$$

From (16) we obtain the RMS value of the sinusoidal signal v(t) defined in (2), given by equation (17)

$$V_{RMS} = \frac{|X|}{4} \tag{17}$$

3. Statement of the problem

This section analyzes the error of the algorithm to calculate the RMS voltage of the line, using the SAL and CAL filters due to a frequency variation in the grid, given by the following equation

$$v(t) = 220\sqrt{2} * sin(2\pi(F_L + \alpha)t) \tag{18}$$

Where $F_L = (60 + \alpha)$ Hz, is the frequency of the mains voltage with a nominal mains frequency equal to 60, a variation α and an RMS amplitude of 220V.

Using (18) and the procedure described above, we find the magnitude and phase variation of phasor X, for a fixed sampling frequency $Fs = 240Hz$ y $\alpha = \pm 1Hz$, with respect to the number of frames, where a frame is defined by a set of four samples taken sequentially. The simulation results are shown in Fig. 1.a and 1.b respectively.
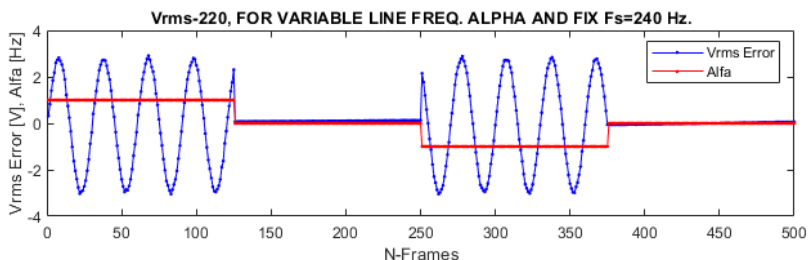

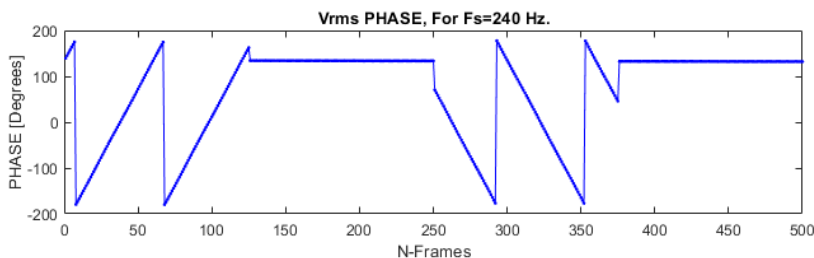**Figure 1.a** Amplitude variation of RMS voltage

Figure 1.b Phase variation of RMS voltage

From Fig.1.a, we observe that the variation of the magnitude V_{RMS} of X is periodic, with a variation $\Delta v = \pm 3v$ Therefore, the RMS value is given by the following equation

$$V_{RMS} = 220 \pm 3v. \tag{19}$$

From Figure 1.b we observe that the variation of the phase of X is linear with respect to the variation of the frequency α and is defined by the following equation

$$M = \phi_{n-}\phi_{n-1} \tag{20}$$

The Table 1, shows the variations of V_{RMS} and M for values of $-1 \leq \alpha \leq +1$, which correspond to a range of grid frequency variations $59 \leq F_L \leq 61\ Hz$.

Table 1. Variations of V_{RMS} and M for values of $-1 \leq \alpha \leq +1$ and $F_S = 240\ Hz$

α	F_L[Hz]	Min Error [V_{RMS}]	Max Error [V_{RMS}]	M [deg/frame]
1.0	61.0	2.9728	2.7844	6.0
0.5	60.5	1.4627	1.4156	3.0
0.0	60.0	0.0	0.0	0.0
-0.5	59.5	1.4433	1.4142	-2.99
-1.0	59.0	2.9674	2.7791	-5.99

From the first and fourth columns of Table 1, a linear relationship between the phase variation M and the frequency variation α can be derived and is given by the following equation:

$$M = 6 * \alpha \tag{21}$$

Therefore, the objective of the regulator described in the next section is to achieve a slope M=0, thus satisfying (6).

4. Regulator design

This section presents the design of the regulator to obtain a phase variation of X equal to zero, which allows the RMS value to be calculated more accurately.

A Timer module (TMR1), implemented in all PIC microprocessors, is used to generate the sampling frequency, which generates an overflow interrupt every $T_S = 1/F_S$. The block diagram of this module is shown in Figure 2.0.
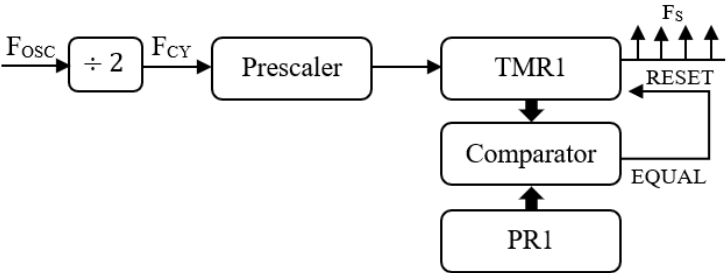
Figure 2. Simplified block diagram of the timer for sample time generation.

From Figure 2.0 the selected oscillator frequency is $F_{OSC} = 20\,MHz$ and a prescaler value of 1. Table 2, shows the PR1 register values for each line frequency with $PR1_0 = 41666$ being the value corresponding to a line frequency of 60 Hz and a sampling frequency of $F_S = 240Hz$.

Table 2. Values of register PR1 for $F_S = 4*F_L$

α	F_L[Hz]	F_S[Hz]	PR1	ΔR
1.0	61.0	244	40983	-683
0.0	60.0	240	41666	0
-1.0	59.0	236	42373	707

From Table 2, we observe that when there is a positive change of α it corresponds to a decrease in the value of PR1 of $\Delta R = -683$. Likewise, for a negative change of α corresponds to an increase of $\Delta R = +707$. These are the minimum and maximum values of the variations that we must use to regulate the sampling frequency.

The implementation of the regulator is shown in Fig.3.0, which "follows" the variations of F_L, to generate the correct sampling frequency F_s , which is used to change the sampling time of the SAL and CAL filters.

To achieve this objective the regulator; using a PI controller, generates the values of ΔR to modify the value of the PR1 register of the timer and thus obtain a new sampling frequency F_S that complies with the relation expressed in (6), taking the value of M to zero [13]. In this way F_S follows the variations of F_L, and using the SAL and CAL filters, we obtain accurate values of V_{RMS}.
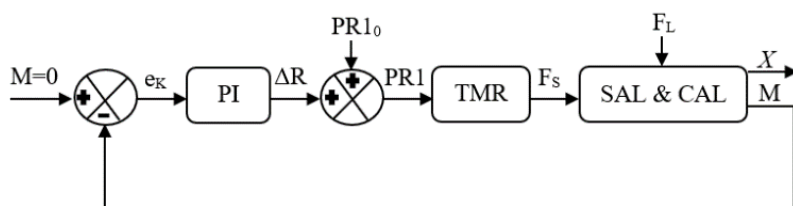
Figure 3. Block diagram of the regulator

The discrete PI controller is given by the equation (22)

$$C(z) = \frac{u(z)}{e(z)} = K * \frac{z}{z-1} \tag{22}$$

The difference equation for (22) is given by the following equation

$$u_k = u_{k-1} + K * e_k \tag{23}$$

5. Results

Simulations have been performed on a personal computer equipped with Intel (R) Core (TM) i5-8265U CPU @ 1.60 GHz 1.80 GHz processor with 8.00 GB RAM with

MATLAB scientific software version 2018th, for a value of $K = 50$ and line frequency variations $\alpha = \pm 1$, which corresponds to frequency variations between 61 and 59 Hz respectively. The results of this simulation are shown in Table 3 and Figure 4.0.

Table 3. Results of regulator implementation

α	F$_L$[Hz]	V$_{RMS}$[V]	ΔR	F$_{EST}$[Hz]
1.0	61.0	220.063	683.22	61.001
0.0	60.0	220.00	0.77	60.00
-1.0	59.0	220.063	706.73	59.002
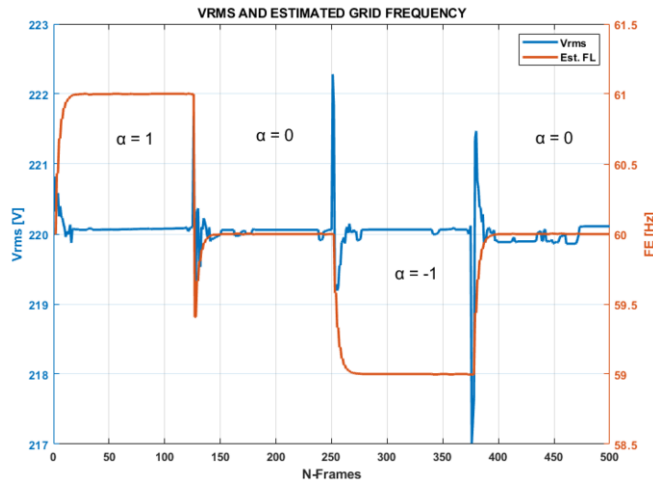
Fig.4. Estimated RMS voltage and line frequency

From the Table 3, we can obtain the percentage error obtained by the algorithm, for the RMS value and the frequency of the estimated grid, is given by

$$error_{RMS} = 0.03\%$$

$$error_{frec} = 0.003\%$$

6. Conclusions

The SAL and CAL filters used in this work are easy to implement since only additions and subtractions are required, i.e., they do not require a high computational load, therefore, they can be implemented in microcontrollers of any spectrum and low cost.

The SAL and CAL filters can be used to calculate the phasors of a sinusoidal signal and with them calculate the RMS value with high accuracy, when the frequency of the signal does not present variations. The algorithm presents errors in the calculation of the RMS value, in situations in which the frequency of the signal varies

The addition of a regulator, to the algorithm that calculates the RMS value of the signal, allows accurate values to be obtained even when the signal frequency varies.

Since the period of the line is proportional to the values of the PR1 register of the timer, this tracking algorithm also allows us to estimate the frequency of the line.

References

[1] Kang S, Yang S, Kim H. Non-intrusive voltage measurement of ac power lines for smart grid system based on electric field energy harvesting. IET, Electronics Letters. 2017. 53(3): 181-183.

[2] Huang TD, Wang WS, Lian KJ. A New Power Signature for Nonintrusive Appliance Load Monitoring. *IEEE Trans. Smart Grid*. 2015. 6(4):1994-1995.

[3] Yu L, Li H, Feng X, Duan J. Nonintrusive appliance load monitoring for smart homes: recent advances and future issues. *IEEE Instrum. Meas. Magazine*. 2016. 19(3):56-62.

[4] Ruuskanen V., Koponen J, Kosonen A, Hehemann M, Keller R, Niemelä M, Ahola J. Power quality estimation of water electrolyzers based on current and voltage measurements. Journal of Power Sources, (2020). 450: 227603.

[5] Mujumdar UB, Joshi JS. Microcontroller based true RMS current measurement under harmonic conditions. 2010. IEEE International Conference on Sustainable Energy Technologies (ICSET): 1-5.

[6] Eski A, Zavalani O, Komici D. RMS Value Measurement Using a Meter Based on ARM Cortex-MO Microprocessor. European Journal of Electrical Engineering and Computer Science. 2017. 1(2).

[7] Gómez EJ, Plazas DC, Restrepo M.F. Voltimetro true-rms sobre fpga basado en algoritmo cordic. Tecnura: Tecnología y Cultura Afirmando el Conocimiento. 2015. 19(2): 129-136.

[8] M. M. Zaid, M. Nauman, M. Rahim, and M. U. Malik, "DSP BASED ENERGY MONITORING WITH ONLINE DAQ SYSTEM.," Acta Tech. Corvininesis - Bull. Eng., vol. 11, no. 2, pp. 59–64, 2018.

[9] J. Barros and E. Pérez, "Automatic detection and analysis of voltage events in power systems," IEEE Trans. Instrum. Meas., vol. 55, no. 5, pp. 1487–1493, Oct. 2006, doi: 10.1109/TIM.2006.881584.

[10] F. Fortes and V. Fialho, "Smart energy meter for iot applications," Int. J. Innov. Technol. Explor. Eng., vol. 8, no. 11, pp. 2708–2712, Sep. 2019, doi: 10.35940/ijitee.K2168.0981119.

[11] Schweitzer EO, Aliaga A. Digital programmable time-parameter relay offers versatility and accuracy. IEEE Transactions on Power Apparatus and Systems. 1980. 1: 152-157

[12] Hazra, L., & Mukherjee, P. (2018). Walsh Functions. In SpringerBriefs in Applied Sciences and Technology (pp. 1–15). Springer Verlag. https://doi.org/10.1007/978-981-10-2809-0_1.

[13] Åström KJ, Hägglund T. The future of PID control. Control engineering practice. 2001. 9(11):1163-1175.